

bitals, as compared with the availability in Nb₂Se (Conard, Norrby & Franzen, 1969) and Ta₂S, results in greater involvement of the chalcogen orbitals in bonding in class II compounds.

The coordination of the sulfur atom in Ta₆S can be described as a distorted capped trigonal prism, a very common coordination of sulfur in metal-rich sulfides. Six of the Ta atoms can be described as forming a slightly distorted trigonal prism with an average Ta-S distance of 2.48 (6) Å; the seventh Ta atom, Ta(2), is off one of the rectangular faces at a distance of 2.53 Å.

In summary, the Ta₆S structure exhibits linear metal clusters similar to those found in Ta₂S and sulfur coordination similar to that found, for example, in V₃S. The absence of significant holes in the structure puts it in a class with V₃S and Nb₂₁S₈, a class to which it also belongs by virtue of containing a group VB metal, by virtue of the sulfur coordination, and by virtue of being more metal rich than Ta₂S. It is suggested that this class of structures differs from the class containing Ta₂S and Nb₂Se primarily in the difference in chalcogen valence, and that the crystallographic holes in Ta₂S and Nb₂Se are, in fact, not 'holes' at all, but are rather regions containing electrons in non-bonding orbitals.

The authors express their appreciation to J. Benson for his assistance in obtaining data from the automated

diffractometer and to H. Baker for taking photographs of the single crystal.

References

- BUSING, W. R. & LEVY, H. A. (1957). *Acta Cryst.* **10**, 180.
 BUSING, W. R., MARTIN, K. O. & LEVY, H. A. (1962). Oak Ridge National Laboratory Report ORNL-TM-305.
 BUSING, W. R., MARTIN, K. O. & LEVY, H. A. (1964). Oak Ridge National Laboratory Report ORNL-TM-306.
 CONARD, B. R., NORRBY, L. J. & FRANZEN, H. F. (1969). *Acta Cryst.* **B25**, 1729.
 DAHM, D. J., BENSON, J. E., NIMROD, D. M., FITZWATER, D. R. & JACOBSON, R. A. (1967). USAEC Report IS-1701.
 FRANZEN, H. F., BEINEKE, T. A. & CONARD, B. R. (1968). *Acta Cryst.* **B24**, 412.
 FRANZEN, H. F. & SMEGGIL, J. G. (1969). *Acta Cryst.* **B25**, 1736.
 HAMBLING, P. G. (1953). *Acta Cryst.* **6**, 98.
 HANSEN, H. P., HERMAN, F., LEA, J. D. & SKILLMAN, S. (1964). *Acta Cryst.* **17**, 1040.
International Tables for X-ray Crystallography (1962). Vol. III, p.216. Birmingham: Kynoch Press.
 JOHNSON, C. K. (1965). Oak Ridge National Laboratory Report ORNL-3794.
 OWENS, J. P., CONARD, B. R. & FRANZEN, H. F. (1967). *Acta Cryst.* **23**, 77.
 PEDERSEN, B. & GRØNVOLD, F. (1959). *Acta Cryst.* **12**, 1022.
 SLATER, J. C. (1964). *J. Chem. Phys.* **41**, 3199.
 WOOLFSON, M. M. (1961). *Direct Methods in Crystallography*. Oxford: Clarendon Press.

Acta Cryst. (1970). **B26**, 129

Neutron Diffraction Study of α -Uranium at Low Temperatures*

BY G. H. LANDER AND M. H. MUELLER

Metallurgy Division, Argonne National Laboratory Argonne, Illinois 60439, U.S.A.

(Received 30 January 1969)

Neutron diffraction measurements have been made on two single crystals of α -uranium in the temperature range 10°K to room temperature. The previously reported variations in the y -positional parameter of the uranium atom are confirmed. There is no deviation from the orthorhombic structure nor any magnetic ordering at low temperature. At low temperature, the increases in the strong nuclear intensities, which are as great as 45% in some cases, are due to a change in the extinction parameter. This effect, observed at various neutron wavelengths, is related to the size of the perfect domains in the crystal and is reversible.

Introduction

Previous diffraction studies on α -uranium near helium temperatures have been confined to zone scans, primarily aimed at studying changes in the unit-cell di-

mensions and y -positional parameter of the uranium atom. These properties were comprehensively examined by Barrett, Mueller & Hitterman (1963) who also reported additional reflections at low temperatures that were possible indications of magnetic ordering. Subsequent susceptibility measurements by Ross & Lam (1968) showed that no simple magnetic ordering exists in α -uranium, although their experiments do not

* Work performed under the auspices of the U.S. Atomic Energy Commission.

exclude a chromium-like spin-density wave. Recent measurements of the elastic moduli (Fisher & Dever, 1968) and thermal expansion (Andres, 1968; Hough, Marples, Mortimer & Lee, 1968) all indicate a so-called transition at $\sim 43^\circ\text{K}$ but the exact nature of the transition has not been established.

α -Uranium has the $A20$ structure of which it is the prototype. The symmetry is orthorhombic C -face centered ($Cmcm$, space group 63) with four atoms per unit cell. The uranium atoms are at the positions $(0, y, \frac{1}{4})$, $(0, \bar{y}, \frac{3}{4})$, $(\frac{1}{2}, \frac{1}{2} + y, \frac{1}{4})$, and $(\frac{1}{2}, \frac{1}{2} - y, \frac{3}{4})$. At room temperature the unit-cell dimensions are $a = 2.854$, $b = 5.870$, and $c = 4.955$ Å, and the y -positional parameter of the uranium atom is $y = 0.1025 \pm 2$. The volume of the unit cell and the y parameter both have minimum values near 40°K . Barrett, Mueller & Hitterman (1963) reported the following values at 40°K , $a = 2.836$, $b = 5.867$, $c = 4.936$ Å and $y = 0.1017 \pm 2$. Although Fisher & Dever (1968) have discussed changes in physical properties in terms of a structural transformation from α to α_0 , no crystallographic evidence for such a transition has been presented. A modest change in the value of the y -positional parameter does not, in crystallographic terms, constitute a change in the structure.

This paper reports the results of neutron diffraction measurements on two single crystals of α -uranium. Three-dimensional data have been collected at room temperature, 80, 45, and 11°K . Selected reflections were measured at intermediate temperatures. Two neutron wavelengths have been used to examine the extinction parameter.

Experimental procedure

The single crystals used in this experiment were provided by E. S. Fisher of this Laboratory. Crystal 1 was

a rectangular parallelepiped with the faces cut perpendicular to the three crystallographic axes. The dimensions along the a , b , and c axes were 1.63, 3.40 and 4.02 mm respectively; the weight of the crystal was 0.466 g. Although the absorption of uranium is small ($\mu = 0.3 \text{ cm}^{-1}$), large variations occur in the lengths of the paths of the neutron beams through the crystal. Therefore, the shape and size of this crystal are not ideal for the collection of accurate integrated intensities. For example, if the incident beam is parallel to the $[100]$ axis, the path length is half as long as that when the incident

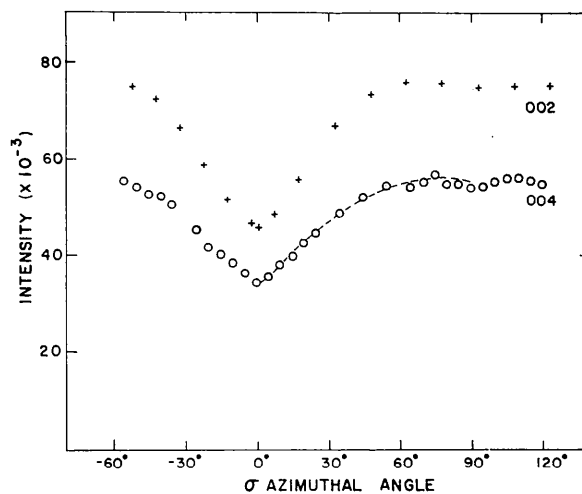


Fig. 1. The variation of the integrated intensities of the 002 and 004 reflections as a function of σ , the angle of rotation about the scattering vector. Crystal 1, $\lambda = 1.575$ Å. The dashed line is the relative variation of the 004 intensity calculated with an absorption coefficient of 4.0 cm^{-1} , and normalized to the observed intensity at $\sigma = 90^\circ$. The position of maximum neutron path length has been chosen to coincide with $\sigma = 0^\circ$.

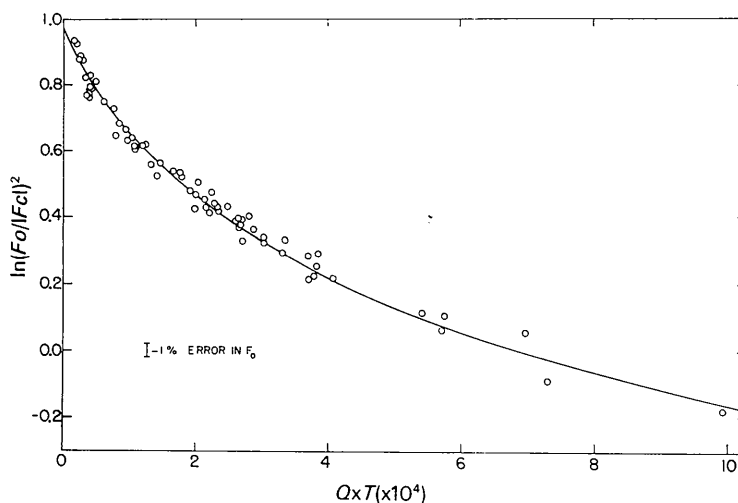


Fig. 2. Plot of $\ln(F_0/F_c)^2$ versus $Q \times T$ for crystal 1, room temperature data. The intercept represents $2 \ln K$, where K is the scale factor. The solid line shows the variation in $\ln(F_0/F_c)^2$ using $(r^*/\lambda) = 4.2 \times 10^3$.

beam is perpendicular to the [100] axis. Serious extinction and multiple scattering effects may, therefore, be expected. On the other hand, high intensities, and thus large crystals, are required if weak extra reflections are found resulting from either a small distortion from the orthorhombic symmetry or from magnetic ordering.

A monochromatic beam of neutrons was obtained from the (111) planes of a germanium crystal used in transmission. The contributions of multiple scattering to the systematically absent 222 reflection were minimized by rotating the monochromator crystal about the scattering vector. Integrated intensities were obtained with a modified 4-circle instrument, the cryo-orienter. This assembly, as previously described (Heaton, Mueller & Hitterman, 1968), permits the examination of approximately 75% of reciprocal space when the sample is in a cryostat. The sample was fastened to a vanadium pin with a small amount of epoxy resin, and the pin screwed to a relatively large copper block. Capsulated heating units were embedded in the copper block, and calibrated platinum and germanium sensors were attached to the periphery of the block to measure the temperature. The sample was cooled with helium exchange gas, which was in contact with the helium reservoir. By the use of an automatically controlled heat input unit and adjusting the pressure of the exchange gas, the temperature was readily controlled to 0.3 K°, with an absolute accuracy of ± 1 K°. The lowest temperature attained with the present exchange gas system was 10°K. This was sufficient for the present experiment, but modifications have been made that will allow helium temperatures to be attained. With the cryo-orienter assembly, the crystal may be rotated $\pm 30^\circ$ about the scattering vector (σ -scan),

for any reflection. This is particularly useful in the examination of multiple scattering.

Results

Crystal 1, $\lambda = 1.575 \text{ \AA}$

After an initial examination of crystal 1 on a standard 4-circle diffractometer, the crystal was transferred to the cryo-orienter assembly, and examined at various temperatures with an incident neutron wavelength of 1.575 Å. This rather long wavelength was chosen to minimize multiple scattering effects. In previous diffraction experiments with α -uranium, a number of weak reflections were observed that are not permitted by the space group. However, these reflections may have been a result of multiple scattering or $\lambda/2$ contamination. The $\lambda/2$ component in the present experiment was minimized by using the 111 reflection of germanium, rotated to eliminate multiple scattering. The $\lambda/3$ component, which is not negligible for a wavelength of 1.575, may be satisfactorily eliminated by using a ^{239}Pu filter that has an absorption edge at 0.53 Å.

At room temperature only those reflections defined by the α -uranium structure were found. Since the shape of crystal 1 is asymmetric, the large variations in the path lengths will give rise to varying extinction effects. This is well illustrated in Fig. 1 where the variations of the 002 and 004 integrated intensities are plotted as a function of σ , which is the angle of rotation about the scattering vector. The position of maximum path length for the neutron beam corresponds to $\sigma = 0^\circ$. Similar variations in other crystals have been reported, for example Willis (1962), which illustrate the path-length dependence of extinction. The relative variation in intensity may be described by calculating

Table 1. Results of least-squares refinements of data from crystal 1 ($\lambda = 1.027 \text{ \AA}$) collected at different temperatures

K is the scale factor, $F_o = K \times |F_c|$, y is the y -positional parameter of the uranium atom. U_a , U_b and U_c are the radii of the thermal ellipsoid of the uranium atom along the a -, b -, and c -axis directions, respectively. R is based on unit weighting, R_w on a weighting scheme with $W = 1/\sigma^2$. The anisotropic thermal ellipsoids from (1) were used in (2) with no extinction parameter.

| | Room temperature | | Temperature | |
|------------------------------|------------------|----------------|----------------|----------------|
| | (1) | (2) | 80°K | 11°K |
| K | 1.62 \pm 2 | 1.21 \pm 2 | 1.63 \pm 3 | 1.59 \pm 4 |
| y | 0.1025 \pm 2 | 0.1026 \pm 7 | 0.1016 \pm 2 | 0.1019 \pm 3 |
| U_a | 83 \pm 2 | 83 | 38 \pm 5 | 36 \pm 7 |
| U_b (10^3 \AA) | 63 \pm 5 | 63 | 0 \pm 10 | 0 \pm 10 |
| U_c | 69 \pm 3 | 69 | 27 \pm 8 | 46 \pm 6 |
| $r^*/\lambda(10^{-3})$ | 4.2 \pm 3 | 0 | 4.2 \pm 3 | 2.4 \pm 3 |
| R | 0.013 | 0.091 | 0.014 | 0.018 |
| R_w | 0.016 | 0.104 | 0.019 | 0.027 |

| Correlation matrix | | | | | | |
|--------------------|-----|------|-------|-------|-------|-------|
| | K | y | U_a | U_b | U_c | r^* |
| K | 1 | 0.06 | 0.61 | 0.50 | 0.67 | 0.95 |
| y | | 1 | 0.07 | 0.06 | 0.08 | 0.04 |
| U_a | | | 1 | 0.28 | 0.55 | 0.43 |
| U_b | | | | 1 | 0.26 | 0.39 |
| U_c | | | | | 1 | 0.51 |
| r^* | | | | | | 1 |

Table 2. *Observed and calculated structure factors at room temperature and 11° K, (crystal 1, $\lambda=1.027$ Å)*The term γ is the calculated ratio of the reflection intensity with and without extinction. For other parameters see Table 1.

| <i>hkl</i> | <i>T</i> (cm) | Room temperature | | | 11°K | | |
|------------|------------------|----------------------------------|--------------------------------|---------------------|----------------------------------|--------------------------------|---------------------|
| | | <i>F</i> ₀ / <i>K</i> | $r^*/\lambda=4200$ γ | $ F_c\gamma^{1/2} $ | <i>F</i> ₀ / <i>K</i> | $r^*/\lambda=2380$ γ | $ F_c\gamma^{1/2} $ |
| 200 | 0.295 | 2.02 | 0.38 | 1.96 | 2.34 | 0.46 | 2.26 |
| 400 | 0.199 | 2.02 | 0.60 | 2.02 | 2.54 | 0.62 | 2.55 |
| 110 | 0.348 | 1.49 | 0.33 | 1.52 | 1.77 | 0.41 | 1.73 |
| 310 | 0.238 | 1.83 | 0.59 | 1.79 | 2.18 | 0.65 | 2.12 |
| 220 | 0.284 | 0.81 | 0.85 | 0.86 | 0.93 | 0.89 | 0.90 |
| 420 | 0.193 | 0.71 | 0.94 | 0.70 | 0.89 | 0.94 | 0.90 |
| 330 | 0.229 | 0.91 | 0.87 | 0.94 | 1.03 | 0.90 | 1.07 |
| 240 | 0.272 | 1.84 | 0.52 | 1.84 | 2.19 | 0.59 | 2.15 |
| 350 | 0.222 | 2.02 | 0.56 | 2.05 | 2.55 | 0.59 | 2.55 |
| 111 | 0.259 | 1.42 | 0.49 | 1.40 | 1.60 | 0.59 | 1.55 |
| 311 | 0.242 | 1.46 | 0.70 | 1.46 | 1.71 | 0.75 | 1.71 |
| 221 | 0.286 | 1.96 | 0.42 | 1.95 | 2.35 | 0.50 | 2.27 |
| 421 | 0.195 | 1.94 | 0.62 | 1.95 | 2.44 | 0.64 | 2.46 |
| 131 | 0.247 | 1.99 | 0.41 | 1.96 | 2.27 | 0.50 | 2.25 |
| 331 | 0.231 | 2.01 | 0.55 | 1.99 | 2.44 | 0.60 | 2.40 |
| 241 | 0.275 | 1.34 | 0.69 | 1.36 | 1.58 | 0.74 | 1.59 |
| 351 | 0.224 | 0.25 | 0.99 | 0.21 | 0.28 | 0.99 | 0.20 |
| 002 | 0.168 | 1.96 | 0.37 | 2.05 | 2.12 | 0.47 | 2.30 |
| 202 | 0.280 | 1.99 | 0.41 | 2.01 | 2.36 | 0.49 | 2.34 |
| 402 | 0.207 | 1.96 | 0.60 | 1.99 | 2.47 | 0.62 | 2.52 |
| 112 | 0.207 | 1.80 | 0.47 | 1.80 | 2.01 | 0.57 | 2.03 |
| 312 | 0.250 | 1.78 | 0.59 | 1.76 | 2.14 | 0.65 | 2.11 |
| 022 | 0.165 | 0.85 | 0.86 | 0.86 | 0.92 | 0.90 | 0.92 |
| 222 | 0.273 | 0.81 | 0.86 | 0.81 | 0.92 | 0.90 | 0.90 |
| 132 | 0.206 | 1.02 | 0.82 | 1.03 | 1.08 | 0.88 | 1.08 |
| 332 | 0.239 | 0.91 | 0.87 | 0.93 | 1.03 | 0.90 | 1.07 |
| 242 | 0.269 | 1.84 | 0.53 | 1.84 | 2.16 | 0.60 | 2.16 |
| 352 | 0.231 | 2.02 | 0.55 | 2.02 | 2.51 | 0.59 | 2.51 |
| 262 | 0.267 | 1.64 | 0.61 | 1.69 | 2.06 | 0.66 | 2.06 |
| 113 | 0.194 | 1.56 | 0.65 | 1.55 | 1.71 | 0.74 | 1.71 |
| 313 | 0.259 | 1.42 | 0.71 | 1.42 | 1.66 | 0.75 | 1.68 |
| 023 | 0.167 | 2.22 | 0.49 | 2.16 | 2.41 | 0.58 | 2.44 |
| 223 | 0.249 | 2.05 | 0.49 | 2.04 | 2.36 | 0.56 | 2.36 |
| 133 | 0.193 | 2.16 | 0.51 | 2.11 | 2.41 | 0.59 | 2.41 |
| 333 | 0.247 | 1.94 | 0.56 | 1.93 | 2.36 | 0.60 | 2.37 |
| 043 | 0.170 | 1.46 | 0.75 | 1.47 | 1.62 | 0.81 | 1.64 |
| 243 | 0.248 | 1.35 | 0.73 | 1.35 | 1.58 | 0.78 | 1.59 |
| 153 | 0.198 | 0.29 | 0.99 | 0.23 | 0.35 | 0.99 | 0.20 |
| 263 | 0.254 | 1.50 | 0.68 | 1.53 | 1.79 | 0.73 | 1.82 |
| 004 | 0.174 | 2.19 | 0.49 | 2.23 | 2.43 | 0.59 | 2.52 |
| 204 | 0.246 | 2.06 | 0.49 | 2.08 | 2.40 | 0.56 | 2.44 |
| 114 | 0.192 | 1.92 | 0.58 | 1.90 | 2.15 | 0.67 | 2.16 |
| 314 | 0.265 | 1.71 | 0.60 | 1.71 | 2.04 | 0.65 | 2.09 |
| 024 | 0.172 | 0.85 | 0.91 | 0.85 | 0.95 | 0.93 | 0.91 |
| 224 | 0.241 | 0.79 | 0.90 | 0.78 | 0.91 | 0.92 | 0.90 |
| 134 | 0.193 | 0.99 | 0.86 | 1.01 | 1.09 | 0.91 | 1.08 |
| 334 | 0.251 | 0.87 | 0.87 | 0.89 | 1.01 | 0.90 | 1.05 |
| 044 | 0.175 | 2.06 | 0.60 | 2.01 | 2.29 | 0.68 | 2.29 |
| 244 | 0.242 | 1.86 | 0.58 | 1.85 | 2.20 | 0.64 | 2.19 |
| 154 | 0.201 | 2.23 | 0.54 | 2.17 | 2.60 | 0.60 | 2.59 |
| 064 | 0.187 | 1.80 | 0.67 | 1.80 | 2.12 | 0.72 | 2.15 |
| 115 | 0.196 | 1.55 | 0.72 | 1.54 | 1.74 | 0.78 | 1.72 |
| 025 | 0.179 | 2.20 | 0.55 | 2.18 | 2.46 | 0.64 | 2.50 |
| 225 | 0.240 | 2.06 | 0.54 | 2.04 | 2.38 | 0.60 | 2.38 |
| 135 | 0.196 | 2.19 | 0.57 | 2.16 | 2.46 | 0.64 | 2.44 |
| 045 | 0.183 | 1.42 | 0.78 | 1.42 | 1.64 | 0.83 | 1.62 |
| 245 | 0.242 | 1.29 | 0.76 | 1.30 | 1.59 | 0.79 | 1.58 |
| 155 | 0.206 | 0.26 | 0.99 | 0.22 | 0.31 | 0.99 | 0.20 |
| 065 | 0.197 | 1.58 | 0.72 | 1.59 | 1.84 | 0.77 | 1.85 |
| 006 | 0.193 | 2.14 | 0.55 | 2.19 | 2.51 | 0.62 | 2.52 |
| 206 | 0.252 | 2.02 | 0.53 | 2.01 | 2.46 | 0.58 | 2.40 |
| 116 | 0.206 | 1.86 | 0.63 | 1.85 | 2.16 | 0.70 | 2.13 |
| 026 | 0.190 | 0.80 | 0.92 | 0.79 | 0.96 | 0.94 | 0.89 |
| 226 | 0.252 | 0.73 | 0.91 | 0.73 | 0.91 | 0.93 | 0.87 |
| 136 | 0.208 | 0.93 | 0.88 | 0.95 | 1.07 | 0.91 | 1.05 |
| 046 | 0.196 | 1.92 | 0.63 | 1.91 | 2.26 | 0.69 | 2.24 |
| 027 | 0.208 | 2.03 | 0.58 | 2.03 | 2.41 | 0.64 | 2.40 |

the absorption factors, A , for the crystal as it is rotated about the scattering vector. The curve (dashed line) in Fig. 2, which exactly follows the variation in the 004 intensity, was drawn by calculating the absorption factors for $\mu=4.0 \text{ cm}^{-1}$ and by normalizing the value of $1/A$ at $\sigma=90^\circ$. Secondary extinction may be treated as an absorption process; therefore, this agreement is to be expected for some value of μ , but the increase from 0.3 to 4.0 cm^{-1} , required in the absorption coefficient, is difficult to interpret.

In general, with a large single crystal, variations in the lengths of the paths will give rise to different extinction effects for equivalent reflections. The faces of crystal 1 are cut perpendicular to the three crystallographic axes, and, when mounted along one of these axes, the geometry is such that there are identical path lengths for all reflections in an equivalent set. A careful examination of the orthorhombic symmetry is, therefore, possible without interference from extinction effects. The agreement between equivalent reflections was good, and agreement between the observed and calculated structure factors was obtained by using an extinction parameter (discussed in following section) of $r^*/\lambda=2.5 \times 10^3$. The limitations on determining this factor arise primarily from its high correlation with the overall scale factor, also an unknown, and the small number of reflections that can be examined at a wavelength of 1.575 \AA .

When the crystal was cooled to 11°K , a large increase in the intensity was observed for almost every reflection. As at room temperature, no additional reflections or satellites were found, although a careful

search was made. The agreement between equivalent reflections at 11°K was equally as good as at the higher temperatures, indicating no departure from the orthorhombic symmetry. The diffraction profiles of the nuclear reflections appeared exactly the same as those obtained at room temperature. For the strong reflections, the increases in intensity at low temperature were very large; the 200 reflection, for example, increased 45% from the value at 77°K . Such an increase in intensity could indicate ferromagnetic ordering, but this explanation has been rejected for the following reasons. First, the increases are not a function of the scattering angle but apparently depend upon the initial intensity of the nuclear reflection. Second, the magnetic moment required to account for the increases in the strong reflections exceeds $2 \mu_B$ per uranium atom; this is in direct conflict with the susceptibility measurements. After collecting data at 11°K the crystal was warmed to 45°K . The nuclear intensities then decreased and were comparable with their values at 80°K . Some experimental evidence suggested that the change in the nuclear intensities involved a small amount of thermal hysteresis.

Since the increases in intensity at low temperature were greatest for the strongest reflections, this suggests that some change occurs in the extinction parameter. At this wavelength (1.575 \AA) the strong reflections were reduced in intensity by as much as a factor of three because of the extinction. A subsequent 45% increase in these intensities could, therefore, be accounted for by a modest change in the extinction parameter. Reasonable agreement between the calculated structure factors and those measured at 11°K was obtained using an extinction parameter of $r^*/\lambda=1.7 \times 10^3$.

The long-wavelength data established that the extra reflections reported previously did not arise from the sample. However, the large extinction may be examined more quantitatively at shorter wavelengths, since a greater number of independent reflections can be measured.

Crystal 1, $\lambda=1.027 \text{ \AA}$

With the crystal mounted about the b axis, intensity data were collected at room temperature, 80 and 11°K . The effect of extinction is illustrated in Fig. 2 where, for the room temperature data, $\ln(F_0/F_c)^2$ is plotted against $Q \times T$. The term F_0 is the observed structure factor, in this case $(I_{\text{obs}} \times \sin 2\theta \times 10^{-4})^{1/2}$, and Q is the usual

crystallographic quantity given by $Q = \frac{\lambda^3}{V^2} \frac{|F_c|^2}{\sin 2\theta}$, where λ is the neutron wavelength, V is the volume of the unit cell, F_c is the calculated structure factor, and 2θ is the scattering angle. The path length, T , was calculated by using a modified version of the Busing & Levy absorption program. Following Zachariasen (1967) $T = - (1/A) \frac{dA}{d\mu}$, where A is the absorption factor. The inter-

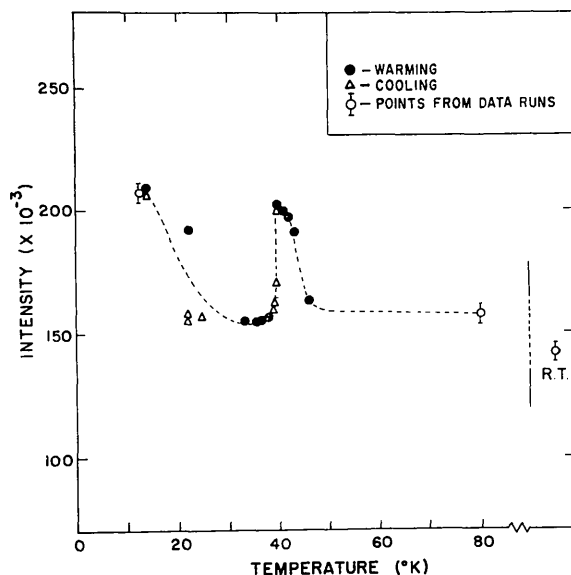


Fig. 3. The variation with temperature of the integrated intensity of the 200 reflection, (crystal 1, b axis mounting, $\lambda=1.027 \text{ \AA}$, $2\theta=43^\circ$). On this scale the calculated intensity of 200, assuming no extinction, is 375×10^3 . The dashed line has been drawn to connect the points and has no theoretical significance.

cept at $Q=0$ is related to the scale factor. If no extinction is present, the points in Fig. 2 should be scattered about a horizontal line.

A least-squares refinement of these data immediately gave a negative temperature factor, a further indication of extinction.

Extinction

The reduction in scattered intensity from the predictions of the kinematical theory is an important feature of the experiments with α -uranium. In an attempt to account for the extinction, we have followed Zachariasen (1967, 1968*a,b*). As a first approximation, primary extinction is neglected. Single crystals of α -uranium are far from perfect. Etching indicates a high dislocation density and the diffraction profiles are broad. The fine structure in the diffraction profiles may be seen with good resolution.

From Zachariasen [(1968*a*) equation (1)] the integrated intensity is reduced by the factor

$$\gamma = \frac{1}{(1+2x)^{1/2}}$$

(we have used γ rather than y to avoid confusion with the positional parameter of the uranium atom)

$$\text{where } x = (r^*/\lambda)QT \text{ and } r^* = \frac{r}{[1 + (r/\lambda g)^2]^{1/2}} \quad (1)$$

(the polarization factors are unity for neutron diffraction). The derivation assumes that the perfect crystal domains have a mean radius r , and that the orientations of the domains obey a Gaussian distribution law in which g is related to the half-width ($\Delta_{1/2} = 0.332/g$).

After obtaining the necessary derivatives the quantity r^* may be included as a parameter in the least-squares analysis. The results of this refinement, with the data at various temperatures, are given in Table 1. Also included is the result of a normal least-squares analysis in which the temperature factors have been fixed. As is to be expected from the distribution of points in Fig. 2 the analysis, with no extinction parameter, gives a scale factor too low and a high value for the R -factor. The correlation matrix for the refinement with r^* is included, and, of special importance is the correlation of $+0.95$ between r^* and K , the scale factor.

The result of the refinement of the data taken at 11°K shows a sharp decrease in the extinction param-

eter, thus confirming the observations at the longer wavelength. The calculated and observed structure factors at room temperature and 11°K are given in Table 2. The large changes in the intensity are illustrated in Fig. 3, with the integrated intensity of the 200 reflection shown as a function of temperature.

Coppens & Hamilton (1968) have introduced anisotropic extinction parameters in a modified least-squares program. Our data from crystal 1, measured at three different temperatures, were used in this program; the extinction ellipsoids were constrained to the orthorhombic point-group symmetry of the crystal. The R values obtained for these refinements ranged from 0.011 to 0.025 and are nearly identical to those shown in Table 1 for the isotropic extinction refinements. We have, therefore, found no evidence for any anisotropic extinction.

Crystal 2, $\lambda = 1.027 \text{ \AA}$

One of the main difficulties in interpreting the data from crystal 1 is the calculation of the path lengths appropriate to equation (1). Crystal 2 was chosen specifically to avoid this problem. The crystal was approximately spherical in shape (0.12 cm diameter) and for the path length the value of 0.10 cm has been used for all reflections. The crystal was mounted approximately about the $\langle 121 \rangle$ axis, which allows the maximum number of independent reflections to be examined with the cryo-orienter unit.

The results obtained from the refinements of data at three temperatures are given in Table 3. As with crystal 1, the agreement between equivalent reflections at all temperatures was good, which indicated no departure from the orthorhombic symmetry. The thermal parameters derived from crystal 2 are more reliable than those from crystal 1, since the overall extinction is less, and these parameters will not be influenced by the anisotropy in crystal shape. The largest vibration is along the a axis. Greater anisotropy exists at 11°K than at higher temperatures since the a -axis vibration (U_a) increases while U_b and U_c continue to decrease (Table 3).

The most important feature of these results is that no increase in intensity occurs at low temperatures. However, no appreciable change in the intensity is expected, since γ (the ratio of observed intensity to that expected if no extinction were present) for the strong 200 re-

Table 3. Results of least-squares refinements of data from crystal 2 ($\lambda = 1.027 \text{ \AA}$) collected at different temperatures

| | Room temperature | 80°K | 11°K |
|------------------------------|------------------|----------------|----------------|
| K | 0.684 \pm 6 | 0.577 \pm 6 | 0.577 \pm 6 |
| y | 0.1027 \pm 3 | 0.1017 \pm 3 | 0.1018 \pm 3 |
| U_a | 85 \pm 3 | 52 \pm 4 | 60 \pm 3 |
| U_b (10^3 \AA) | 67 \pm 4 | 41 \pm 5 | 34 \pm 7 |
| U_c | 64 \pm 3 | 40 \pm 5 | 25 \pm 8 |
| $r^*/\lambda(10^{-3})$ | 1.03 \pm 15 | 1.25 \pm 15 | 1.24 \pm 16 |
| R | 0.022 | 0.018 | 0.019 |
| R_w | 0.026 | 0.024 | 0.024 |

The notation is the same as in Table 1.

flexion is as high as 0.8 at room temperature. The intensities of a number of different reflections were examined as the crystal was cooled from 80 to 10 °K. No significant increases in intensity were found in this temperature range.

By increasing the wavelength the extinction may increase sufficiently so that a small *fractional* change in the extinction parameter results in a detectable change in the nuclear intensity. The wavelength was changed to 2.18 Å, the highest value possible with the shielding assembly. Fig. 4 shows the peak intensities of three reflections as a function of temperature. Both the 002 and 200 reflections are strong and show sharp increases at 40 °K. The 020 reflection is weak and hence not greatly affected by any change in the extinction parameter. For the 020 reflection, the variation of the *y*-positional parameter with temperature implies a maximum value for the intensity around 40 °K. A calculation of the approximate extinction parameter for the few reflections examined at this long wavelength gives 0.7×10^3 for r^*/λ .

Discussion

Following Zachariasen (1968*a*) the values of r^* at different wavelengths may be used to determine the r and g parameters for the crystal. According to this theory the relationship $1 \leq (r_1^*/\lambda_1)/(r_2^*/\lambda_2) \leq \lambda_2/\lambda_1$ must hold. For crystal 1, $\lambda_2/\lambda_1 = 1.575/1.027 = 1.535$ and $(r_1^*/\lambda_1)/(r_2^*/\lambda_2) = (4.2 \pm 0.3)/(2.5 \pm 0.3) = 1.7 \pm 0.2$ at room temperature, and $2.4/1.7 = 1.4$ at low tempera-

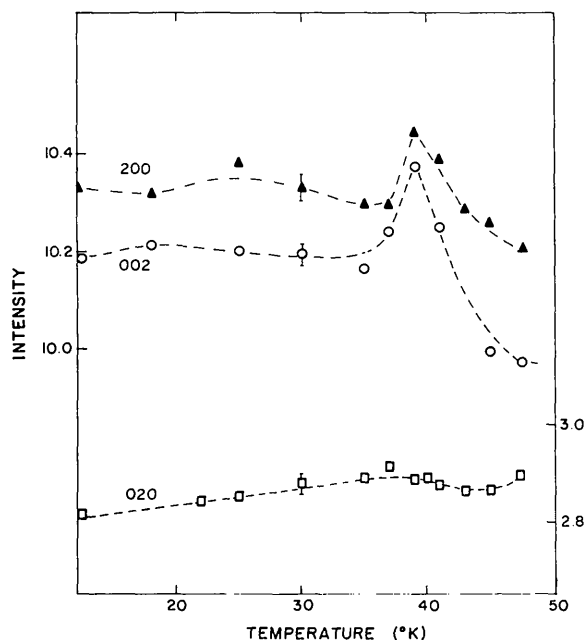


Fig. 4. Variation with temperature of peak intensities of the 200, 020, and 002 reflections for crystal 2 at $\lambda = 2.18$ Å. The scale on the left applies to the 200 and 002 reflections, that on the right to the 020 reflection. The dashed lines have no theoretical significance.

ture. Since r^* rather than (r^*/λ) is more nearly constant, this suggests that the crystals are the so-called type II, for which the diffraction pattern from a single domain is wider than the function describing the distribution of all the domains. The size of the perfect domains, r , is 0.4×10^{-4} cm at room temperature and 0.2×10^{-4} cm at low temperature, and, in both cases, g is greater than 5×10^3 . For crystal 2, r^* is again approximately constant. The ratios $\lambda_2/\lambda_1 = 2.18/1.027 = 2.1$ and $(r_1^*/\lambda_1)/(r_2^*/\lambda_2) = 1.0/0.7 = 1.5$ indicate that, as with crystal 1, the crystal is of type II with $r \approx 0.13 \times 10^{-4}$ cm.

One of the aims of this experiment was to search for anisotropy in the thermal vibrations of the uranium atom. The results presented in Tables 1 and 3 are not entirely consistent. For example, at 80 °K the thermal vibrations in the b direction (U_b), refined with data from crystal 1 (Table 1), appear to vanish. On the other hand, the large extinction effects involved in refining the data at all temperatures from crystal 1 make the values of the thermal parameters inevitably suspect. The results from crystal 2, in which the extinction effects are much smaller, are certainly better behaved and, apparently, a predominant vibration occurs in the [100] direction. This is of particular interest in view of the unusual behavior of the c_{11} elastic modulus reported by Fisher & Dever (1968). The agreement between the two experiments is encouraging. On the other hand, the thermal parameters from the neutron diffraction data have been interpreted in terms of purely harmonic forces. Since negative thermal expansion coefficients below 40 °K are present in uranium, this simple interpretation should be treated as a first approximation.

In this study, we have found considerable evidence that suggests the 'transition' around 40 °K is associated with the physical perfection of the crystal. The crystals are type II, and at low temperatures the size of the perfect domains is reduced, roughly by a factor of two. If the extinction effects are large, when either large crystals or long wavelengths are used, the proportional change in the extinction, resulting from the reduction in the domain size, predicts increases in the intensities of the strong nuclear reflections. The reduction in the domain size is a reversible process, so that when the sample is reheated the domains revert approximately to their original size and the intensities decrease. This appears to be the first observation of such an effect, and we are unable to put forward any simple explanation. The suggestion of Fisher & Devers (1968) and Andres (1968) that a transition from α to an α_0 phase occurs at 43 °K is possible only if the transition involves small changes, and in the present experiment may be inhibited by the crystal imperfections. Neither a change in crystal structure nor any magnetic ordering has been found in α -uranium at low temperature (*i.e.* down to 10 °K). However, in the lanthanide series, certain magnetic properties have indeed been found to vary depending on the purity and physical perfection of the sample, and a similar situation may prevail in the actinide series.

We wish to thank L. Heaton and E. S. Fisher for discussion, H. W. Knott for cutting crystal 2, and R. L. Hitterman for his invaluable assistance in the data collection. We are grateful to C. M. Vincent for help in writing a *SPEAKEASY* program for the least-squares refinement.

References

ANDRES, K. (1968). *Phys. Rev.* **170**, 614.
 BARRETT, C. S., MUELLER, M. H. & HITTERMAN, R. L. (1963). *Phys. Rev.* **129**, 625.

COPPENS, P. & HAMILTON, W. C. (1968). American Crystallographic Association Meeting, Buffalo, New York. Abstract G2.
 FISHER, E. S. & DEVER, D. (1968). *Phys. Rev.* **170**, 607.
 HEATON, L., MUELLER, M. H. & HITTERMAN, R. L. (1968). American Crystallographic Association Meeting, Buffalo, New York. Abstract H3.
 HOUGH, A., MARPLES, J. A. C., MORTIMER, M. J. & LEE, J. A. (1968). *Phys. Letters*, **27A**, 222.
 ROSS, J. W. & LAM, D. J. (1968). *Phys. Rev.* **165**, 617.
 WILLIS, B. T. M. (1962). *Pile Neutron Research in Physics*, p. 455. Vienna: I.A.E.A.
 ZACHARIASEN, W. H. (1967). *Acta Cryst.* **23**, 558.
 ZACHARIASEN, W. H. (1968a). *Acta Cryst.* **A24**, 212.
 ZACHARIASEN, W. H. (1968b). *Acta Cryst.* **A24**, 324.

Acta Cryst. (1970). **B26**, 136

Representation of Phase Probability Distributions for Simplified Combination of Independent Phase Information

BY WAYNE A. HENDRICKSON* AND EATON E. LATTMAN

The Johns Hopkins University, Thomas C. Jenkins Department of Biophysics, Baltimore, Maryland 21218, U.S.A.

(Received 27 January 1969)

The phase probability distributions associated with several types of phase information of possible use in protein structure analysis have been cast in the simplified representation,

$$P(\alpha) = N \exp(A \cos \alpha + B \sin \alpha + C \cos 2\alpha + D \sin 2\alpha).$$

This formulation permits the combination of independent phase information from different sources by simple addition of the constant coefficients A , B , C and D which encode the phase information. Also, use of this form for the phase probability expedites numerical integration of the centroid phase integrals and makes analytic integration possible. In order to achieve the simplified representation for the isomorphous replacement method it was necessary to reformulate the error analysis for that method. A computational comparison of phase determination by various methods for isomorphous replacement substantiates the validity of the new approach.

Introduction

Crystal structure analyses usually proceed, by one means or another, to a trial structure which can then be refined to a best match between the calculated and observed intensities. This is not possible in protein structure analysis for the structural complexity and practical resolution limits make a satisfactory trial structure unobtainable in the early stages. Structural information must be obtained by direct interpretation of the electron density map. It is most important, then, that this Fourier synthesis be as accurate as possible.

Blow & Crick (1959) have shown that the Fourier synthesis with minimal mean-square error is achieved by the use of coefficients defined by the centroid of the structure-factor probability distribution. In practice

this has been reduced to the centroid of the phase probability distribution, assuming the amplitude to be fixed. The resulting Fourier synthesis has as coefficients

$$\xi = F_P \frac{\int_0^{2\pi} \exp(i\alpha) P(\alpha) d\alpha}{\int_0^{2\pi} P(\alpha) d\alpha} \quad (1)$$

where F_P is a structure factor amplitude from the protein crystal and $P(\alpha) d\alpha$ is the probability that its phase angle α be between α and $\alpha + d\alpha$. This formula has been implemented for the isomorphous replacement method by determining the phase probability distribution from the lack of closure errors in phase determinations (Blow & Crick, 1959; Dickerson, Kendrew & Strandberg, 1961; Cullis, Muirhead, Perutz, Rossmann & North, 1961). The extension to phase information from anomalous scattering has been made in a similar way by North (1965) and Matthews (1966).

* Present address: Laboratory for the Structure of Matter, U.S. Naval Research Laboratory, Washington, D.C. 20390, U.S.A.